Springer

Journal of
Mechanical
Science and
Technology

Journal of Mechanical Science and Technology 22 (2008) 871~878

www.springerlink.com/content/1738-494x

A finite element formulation based on an enhanced first order shear deformation theory for composite and sandwich structures

Jinho Oh[1], Maenghyo Cho[1,*], Jun-Sik Kim[2] and Michel Grédiac[3]

[1] *Seoul National University, San 56-1, Shillim-Dong, Kwanak-Gu, Seoul 151-744, Korea*
[2]*The Pennsylvania State University, University Park, PA 16802, U.S.A.*
[3]*Campus de Clermont-Ferrand-Les Cézeaux, BP265-613175 AUBIÈRE CEDEX-France*

(Manuscript Received December 28, 2007; Revised January 4, 2008; Accepted January 4, 2008)

Abstract

A finite element formulation based on an enhanced first order shear deformation theory is developed to accurately and efficiently predict the behavior of laminated composite and sandwich structures. An enhanced first order shear deformation theory is systematically derived by minimizing the least-squared energy error between the first order shear deformable plate theory and a higher order shear deformable plate theory. In this way, the strain energy of a higher order theory is transformed to that of the Reissner-Mindlin plate theory. This minimization procedure yields a relationship between them that is also used to improve the accuracy of predicted stresses and displacements. The key feature of the proposed theory is in that it can be implemented to commercial FEM packages by simply changing the input, and the results obtained can be also enhanced by post-processing them via a differential quadrature method. Thus, a proposed finite element formulation can be widely used in various application problems. Through numerical examples, the accuracy and robustness of the present formulation are demonstrated.

Keywords: Reissner-mindlin plate theory; Enhanced first order shear deformation theory; Laminated composites; Sandwich plates; Stress recovery

1. Introduction

Various analysis models have been developed to predict the behaviors of composite and sandwich structures efficiently and accurately. Among many proposed models, a higher order zig-zag theory [1, 2] is known to be one of the most efficient theories to compute the through-the-thickness distributions of displacements and stresses for laminated composite structures. This higher-order zigzag theory (HOZT) satisfies the continuity condition at interfaces as well as the traction conditions at top and bottom surfaces of transverse shear stresses. It employs the degrees of freedom defined at the reference plane only but produces accurate results as demonstrated in Refs. [1, 2]. However, a higher order zig-zag theory requires C_1 shape functions (slope continuity condition along the boundary of the element) for the finite element realization in general. These shape functions are not available in most commercial finite element packages especially for a shear deformable plate theory. Thus it is difficult to implement a special zigzag plate element with conventional isoparametric elements to those commercial packages. A variational–asymptotic approach based on the first order shear deformation Mindlin-Reissner plate theory was proposed by Yu et al [3].

To overcome this drawback, an enhanced first order shear deformation theory (EFSDT) [4] is developed, which requires C_0 shape functions only for a finite element realization. In this study, we implement an EFSDT to the commercial package (ANSYS) routine. This will improve the prediction of deforma-

*Corresponding author. Tel.: +82 2 880 1693, Fax.: +82 2 886 1693
E-mail address: mhcho@snu.ac.kr
DOI 10.1007/s12206-008-0103-8

tions and stresses through the thickness of plates via postprocessing the results obtained from ANSYS. Through several numerical examples, the accuracy and robustness of the present FE method based on EFSDT are demonstrated.

2 Formulation of an enhanced first order shear deformation theory

In this section, an enhanced first order shear deformation theory is obtained by applying the strain energy transformation to the strain energy of a higher order zig-zag theory. A way to recover the stresses and displacements via the differential quadrature method is then developed, which can be directly applied to the results obtained from the commercial finite element software.

2.1 Displacement formulation

In this paper, a linear elastic plate theory is considered for laminated plates made of a monoclinic material. The reference plane is represented by x_α and the through-the-thickness position is denoted by x_3, where $x_3 \in [-h/2, +h/2]$. As long as the interior solution is concerned, the general form of displacements can be expressed by

$$u_\alpha(x_i) = u^o_\alpha(x_\beta) - u^o_{3,\alpha}(x_\beta)\, x_3 + W_\alpha(x_i) \tag{1}$$

$$u_3(x_i) = u^o_3(x_\beta) + W_3(x_i) \tag{2}$$

in which, u^0_α and u_3 are in-plane and out-of-plane displacements in the reference plane, respectively. $W_\alpha(x_i)$ and $W_3(x_i)$ represent warping functions.

The in-plane displacement fields of the HOZT are constructed by superimposing a linear zig-zag displacement to a smooth globally cubic varying displacement. The final displacement fields are expressed in terms of the five primary degrees of freedom by applying the interface continuity conditions as well as the bounding surface conditions for transverse shear stresses. These are then written as follows:

$$\begin{aligned} u_\alpha = {} & u^o_\alpha - u^o_{3,\alpha} x_3 + x_3^3 \frac{1}{3}\phi_\alpha - \frac{h^2}{4} x_3 \phi_\alpha \\ & - \frac{x_3}{2} \sum_{k=1}^{N-1} a^{(k)}_{\alpha\gamma} \phi_\gamma - x_3^2 \frac{1}{2h} \sum_{k=1}^{N-1} a^{(k)}_{\alpha\gamma} \phi_\gamma \\ & + \sum_{k=1}^{N-1} a^{(k)}_{\alpha\gamma} \phi_\gamma (x_3 - x_3^{(k)}) H(x_3 - x_3^{(k)}) \end{aligned} \tag{3}$$

where $a^{(k)}_{\alpha\gamma}$ are constants and computed from the interface continuity conditions. This is a modified version of the displacement field given in Refs. [1, 2].

The in-plane warping functions can be simply obtained from the in-plane displacements given in Eq. (3), which gives us a good approximation to those of the 3D warping functions. The displacements can be then expressed in compact form

$$\begin{aligned} u_\alpha(x_i) &= u^o_\alpha(x_\alpha) - u^o_{3,\alpha}(x_\alpha) x_3 + \Phi_{\alpha\gamma}(x_3)\phi_\gamma(x_\alpha) \\ u_3(x_i) &= u^o_3(x_\alpha) \end{aligned} \tag{4}$$

where $W_\alpha = \Phi_{\alpha\gamma}(x_3)\phi_\gamma(x_\alpha)$, and $\Phi_{\alpha\gamma}(x_3)$ can be computed from Eq. (3). Subsequently the corresponding in-plane strains are given by

$$\varepsilon_{\alpha\beta}(x_i) = \varepsilon^{(o)}_{\alpha\beta}(x_\alpha) + x_3 \varepsilon^{(1)}_{\alpha\beta}(x_\alpha) + \varepsilon^{(w)}_{\alpha\beta}(x_i) \tag{5}$$

in which the detailed expression of strain components can be found in Ref. [4], and the transverse shear strains are given as

$$\gamma_{3\alpha}(x_i) = u_{\alpha,3} + u_{3,\alpha} = \Phi_{\alpha\gamma,3}(x_3)\phi_\gamma(x_\beta) + W_{3,\alpha} \tag{6}$$

where the warping function W_3 is very small as compared to the effective transverse shear strains, ϕ_γ, for moderately thick plates in general. The transverse shear strains are then approximated as follows:

$$\gamma_{3\alpha} \cong \Phi_{\alpha\gamma,3}(x_3)\phi_\gamma(x_\beta) \tag{7}$$

2.2 Relationship between two plate theories

In order to derive the relationship between the aforementioned two plate theories, one can apply least square minimization to strains and displacements obtained from Reissner-Mindlin theory and the HOZT. Consequently, this can be summarized as follows:

$$\min_{\bar{\varepsilon}^o_{\alpha\beta}} \langle \| \varepsilon_{\alpha\beta} - \bar{\varepsilon}_{\alpha\beta} \|_2 \rangle = 0 \;\rightarrow\; \bar{\varepsilon}^o_{\alpha\beta} = \varepsilon^{(0)}_{\alpha\beta} + \frac{1}{h}\langle \varepsilon^{(w)}_{\alpha\beta} \rangle \tag{8}$$

$$\min_{\kappa_{\alpha\beta}} \langle \| \varepsilon_{\alpha\beta} - \bar{\varepsilon}_{\alpha\beta} \|_2 \rangle = 0 \;\rightarrow\; \kappa_{\alpha\beta} = \varepsilon^{(1)}_{\alpha\beta} + \frac{12}{h^3}\langle x_3 \varepsilon^{(w)}_{\alpha\beta} \rangle \tag{9}$$

$$\min_{\bar{u}^o_\alpha} \langle \| u_\alpha - \bar{u}_\alpha \|_2 \rangle = 0 \;\rightarrow\; \bar{u}^o_\alpha = u^o_\alpha + \frac{1}{h}\langle W_\alpha \rangle \tag{10}$$

$$\min_{\theta_\alpha} \langle \| u_\alpha - \bar{u}_\alpha \|_2 \rangle = 0 \;\rightarrow\; \theta_\alpha = -u^o_{3,\alpha} + \frac{12}{h^3}\langle x_3 W_\alpha \rangle \tag{11}$$

$$\min_{\overline{u}_3^o} \langle \| u_3 - \overline{u}_3 \|_2 \rangle = 0 \;\rightarrow\; \overline{u}_3^o = u_3^o + \frac{1}{h}\langle W_3 \rangle \tag{12}$$

where the averaged in-plane strains, curvatures and displacements are denoted by $\overline{\varepsilon}_{\alpha\beta}$, $\kappa_{\alpha\beta}$ and $\overline{u}_\alpha$, which are taken from Reissner-Mindlin theory. The symbol $\langle \bullet \rangle$ is defined by $\langle \bullet \rangle = \int_{-h/2}^{h/2} \bullet \, dx_3$. These equations, Eqs. (8)-(12), minimize the errors of the in-plane stresses in the least-square sense, which can be also derived by transforming the strain energy of the HOZT into that of Reissner-Mindlin like theory.

The strain energy of the HOZT based on Eq. (4) is written in a compact form.

$$\begin{aligned} 2U \;&= \varepsilon_0^T A \varepsilon_0 + 2\varepsilon_0^T B K_0 + K_0^T D K_0 \\ &+ \phi^T G \phi + 2\varepsilon_0^T E K_h + 2K_0^T F K_h \\ &+ K_h^T H K_h \end{aligned} \tag{13}$$

where stiffness matrices A, B, D, G, E, F, H and strain vectors $\varepsilon_0, K_0, \phi, K_h$ are defined in Ref. [4]. Substituting Eqs. (8)-(12) into the above yields

$$\begin{aligned} 2U = &\left(\overline{\varepsilon}_0 - \tilde{C}\kappa_h\right)^T A \left(\overline{\varepsilon}_0 - \tilde{C}\kappa_h\right) \\ &+ 2\left(\overline{\varepsilon}_0 - \tilde{C}\kappa_h\right)^T B \left(\overline{\kappa}_o - \tilde{\Gamma}\kappa_h\right) \\ &+ \left(\overline{\kappa}_o - \tilde{\Gamma}\kappa_h\right)^T D \left(\overline{\kappa}_o - \tilde{\Gamma}\kappa_h\right) \\ &+ \overline{\gamma}^T \left(\hat{\Gamma}^T \; G\hat{\Gamma}\right)\overline{\gamma} + 2\left(\overline{\varepsilon}_0 - \tilde{C}\kappa_h\right)^T E\kappa_h \\ &+ 2\left(\overline{\kappa}_o - \tilde{\Gamma}\kappa_h\right)^T F\kappa_h + \kappa_h^T H \kappa_h \end{aligned} \tag{14}$$

in which $\tilde{C}$ and $\tilde{\Gamma}$ are the relationship matrices that are associated with $\frac{1}{h}\langle \varepsilon_{\alpha\beta}^{(w)} \rangle$ and $\frac{12}{h^3}\langle x_3 \varepsilon_{\alpha\beta}^{(w)} \rangle$, respectively. After rearranging Eq. (14), one can obtain the energy of Reissner-Mindlin like theory and the truncated energy as follows:

$$2U = \overline{\varepsilon}_0^T A \overline{\varepsilon}_0 + 2\overline{\varepsilon}_0^T B \overline{\kappa}_0 + \overline{\kappa}_0^T D \overline{\kappa}_0 + \overline{\gamma}^T \hat{G} \overline{\gamma} + 2\tilde{U} \tag{15}$$

where the truncated energy $\tilde{U}$ is given by

$$\begin{aligned} 2\tilde{U} = &2\overline{\varepsilon}_0^T \left(-A\tilde{C} - B\tilde{\Gamma} + E\right)\kappa_h \\ &+ 2\overline{\kappa}_0^T \left(-B^T\tilde{C} - D\tilde{\Gamma} + F\right)\kappa_h \\ &+ \kappa_h^T \left(\tilde{C}^T A\tilde{C} + 2\tilde{C}^T B\tilde{\Gamma} - 2\tilde{C}^T E + \tilde{\Gamma}^T D\tilde{\Gamma} - 2\tilde{\Gamma}^T F + H\right)\kappa_h \end{aligned} \tag{16}$$

This truncated energy should be minimized with respect to the relationship matrices to obtain the best approximation to the HOZT. In this way, the strain energy of the HOZT can be successfully expressed in terms of the variables of Reissner-Mindlin theory. Once the relationship matrices are found, which minimize Eq. (16), the effective transverse shear stiffness can be obtained by

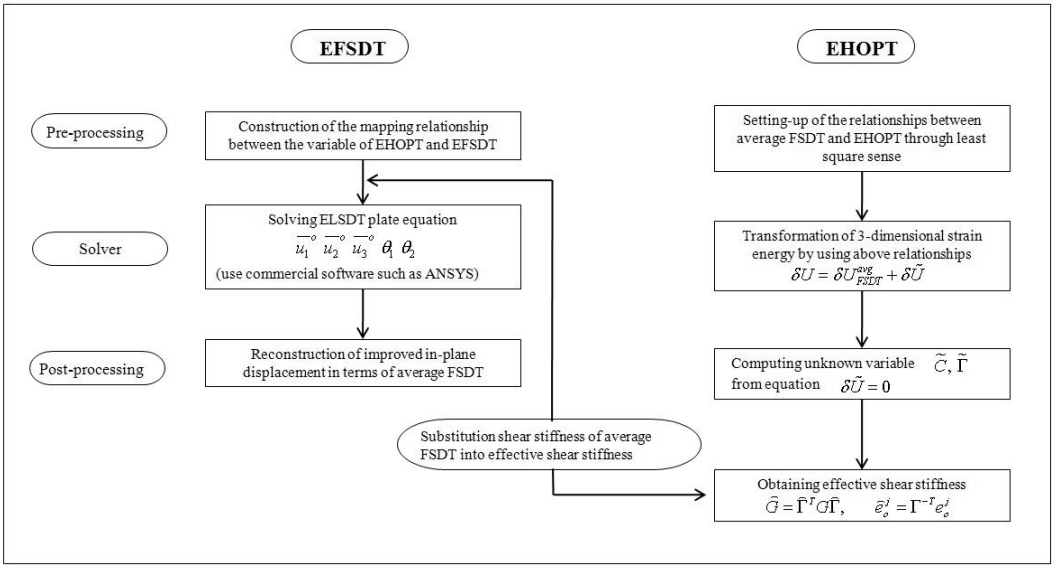

Fig. 1. Flowchart of the enhanced first order shear deformation method.

$$\hat{G} = \hat{\Gamma}^T \; G\hat{\Gamma} \tag{17}$$

where $\hat{\Gamma}$ is the inverse of the sub-matrix of $\tilde{\Gamma}$. Here one can see that an EFSDT is different only from Reissner-Mindlin theory in terms of the shear stiffness matrix. This implies that an EFSDT can be easily implemented to most commercial finite element packages, which have Reissner-Mindlin type elements, with virtually no effort.

2.3 Recovery process

In this subsection, the recovery process using the outputs of commercial finite element packages is described, which improves significantly the predicted displacements and stresses via the relationship between an EFSDT and the HOZT. Explicit relations between the HOZT and Reissner-Mindlin like theory are derived via the strain energy transformation presented in previous section.

In the post-processing phase, one can recover the displacements using the variables of Reissner-Mindlin like theory denoted by the overbars in Eq. (18) as follows:

$$\begin{aligned} u_\alpha &= \bar{u}_\alpha^0 - \bar{u}_{3,\alpha}^0 x_3 - C_{\alpha\gamma}\phi_\gamma + \Phi_{\alpha\gamma}(x_3)\hat{\Gamma}_{\gamma\mu}\bar{\gamma}_{3\mu}, \\ u_3 &= \bar{u}_3^0 \end{aligned} \tag{18}$$

Similarly, the strains are recovered by

$$\begin{aligned} \varepsilon_{\alpha\beta} &= \bar{\varepsilon}_{\alpha\beta}^o - \frac{1}{h}\left\langle \tilde{\Phi}_{\alpha\gamma}^e(x_3)\hat{\Gamma}\bar{\gamma}_{,\beta} \right\rangle \\ \varepsilon_{3\alpha} &= \tilde{\Phi}_{\alpha\beta}^s(x_3)\hat{\Gamma}\bar{\gamma} \end{aligned} \tag{19}$$

in which the values with overbars are obtained from the outputs of the commercial FE software ANSYS.

The derivatives of nodal variables are calculated by using the differential quadrature method [5], which is a simple numerical approach to solve partial differential equations. In this method, the partial derivatives of a function with respect to a variable at any discrete point are approximated by weighted linear sums of the function values at all the discrete points in the overall chosen domain. For instance, the partial derivatives with respect to in-plane coordinates are calculated by

$$f_x^{(n)}(x_i, y_j) = \sum_{k=1}^{N_x} C_{ik}^{(n)} f(x_k, y_j) \quad n = 1, 2, ..., (N_x - 1) \tag{20}$$

$$f_y^{(m)}(x_i, y_j) = \sum_{k=1}^{N_y} \bar{C}_{jk}^{(m)} f(x_i, y_k) \quad m = 1, 2, ..., (N_y - 1) \tag{21}$$

$$\begin{aligned} f_{xy}^{(n+m)}(x_i, y_j) &= \sum_{k=1}^{N_x} C_{ik}^{(n)} \sum_{l=1}^{N_y} \bar{C}_{jl}^{(m)} f(x_k, y_l) \\ i &= 1, 2, ..., N_x \;\; and \;\; j = 1, 2, ..., N_y \end{aligned} \tag{22}$$

where N_x is a grid point x-direction and N_y in the y-direction. The numbers n and m represent the order of the derivatives with respect to x and y direction. $C_{ij}^{(n)}$ and $\bar{C}_{ij}^{(m)}$ are weighting coefficients, which are computed as follows:

$$\begin{aligned} &C_{ij}^{(n)} = n\left(C_{ii}^{(n-1)} C_{ij}^{(1)} - \frac{C_{ij}^{(n-1)}}{x_i - x_j} \right) \\ &for \quad i, j = 1, 2, \ldots, N_x \\ &j \neq i \quad and \quad n = 2, 3, \ldots, N_y - 1 \end{aligned} \tag{23}$$

$$\begin{aligned} &\bar{C}_{ij}^{(m)} = m\left(\bar{C}_{ii}^{(m-1)} \bar{C}_{ij}^{(1)} - \frac{\bar{C}_{ij}^{(m-1)}}{y_i - y_j} \right) \\ &for \quad i, j = 1, 2, \ldots, N_y \\ &j \neq i \quad and \quad m = 2, 3, \ldots, N_y - 1 \end{aligned} \tag{24}$$

$$\begin{aligned} &C_{ii}^{(n)} = -\sum_{j=1,\, j\neq i}^{N_x} C_{ij}^{(n)} \;\; for \quad i, j = 1, 2, \ldots, N_x \\ &and \quad n = 1, 2, 3, \ldots, N_x - 1 \end{aligned} \tag{25}$$

$$\begin{aligned} &\bar{C}_{ii}^{(m)} = -\sum_{j=1,\, j\neq i}^{N_y} C_{ij}^{(m)} \;\; for \quad i, j = 1, 2, \ldots, N_y \\ &and \quad m = 1, 2, 3, \ldots, N_y - 1 \end{aligned} \tag{26}$$

in which

$$C_{ij}^{(1)} = \frac{M^{(1)}(x_i)}{(x_i - x_j) M^{(1)}(x_j)} \quad i, j = 1, 2, \ldots, N_x \;\; but \;\; j \neq i \tag{27}$$

$$\bar{C}_{ij}^{(1)} = \frac{P^{(1)}(y_i)}{(y_i - y_j) P^{(1)}(y_j)} \quad i, j = 1, 2, \ldots, N_y \;\; but \;\; j \neq i \tag{28}$$

A summary of the proposed finite element formulation is given as follows: First, the effective shear stiffness matrix is obtained by using the in-plane warping functions dependent on the layer material and geometric properties taken from the HOZT and applying the strain energy transformation process via the least square minimization. Second, after the shear stiffness is replaced with the effective one, the modeling and analysis of composite and sandwich structures is performed by ANSYS [6]. Lastly, in order to get the detailed through-the-thickness distributions of displacements and stresses, the recovery procedure is

applied to the output of ANSYS, which is carried out by the in-house code. A detailed flowchart of the enhanced first order shear deformation method is given in Fig. 1.

3. Numerical results

The finite element formulation based on an EFSDT is applied to ANSYS. In this commercial software, the SHELL99 element is selected to implement the proposed finite element formulation based on an EFSDT, which utilizes the C_0 - shaped functions. In what follows, it will be demonstrated that the present approach (an EFSDT together with the recovery process) is simple yet accurate throughout the numerical examples.

The ply material properties [7] in cross-ply laminated plates are given as

$$\begin{aligned} &E_L / E_T = 25, G_{LT} / E_T = 0.5, \\ &G_{TT} / E_T = 0.2, \nu_{LT} = \nu_{TT} = 0.25 \end{aligned} \tag{29}$$

where L denotes a fiber direction and T denotes a perpendicular direction to the fiber. For a sandwich plate, the material properties of a face sheet are the same as Eq. (29), and the core material properties [8] are given by

$$\begin{aligned} &E_x = 1.0\times10^8 \,\mathrm{Pa}\left(0.145\times10^5 \,\mathrm{psi}\right),\ E_2 = E_3 \\ &G_{13} = 0.4\times10^8 \,\mathrm{Pa}\left(0.58\times10^4 \,\mathrm{psi}\right), \\ &G_{23} = G_{12} = G_{13},\ \nu_{12} = 0.25 \end{aligned} \tag{30}$$

The length-to-thickness ratio, S, is assumed to be 4 or 10, in which S=4 represents a very thick plate and S=10 does a moderately thick plate. Only two cases are evaluated, since these are challengeable problems due to the significant shear deformation effect, especially for a sandwich plate. The through-the-thickness distributions of in-plane stresses and transverse shear stresses are investigated and discussed, which are important from the strength and stiffness design points of view.

Three cases are considered to assess the accuracy and efficiency of the present approach.

Case (1): An eight-layer rectangular plate [90/0/90/0/0/90/0/90] with simply supported boundary conditions along the edge under the distributed uniform pressure loading. The comparison of center deflections is made in Table 1, where one can confirm that the present approach (i.e., the finite element formulation based on an EFSDT) agrees very well with those of the HOZT. The displacement contour of a rectangular composite plate is plotted in Fig. 2, and the in-plane stress σ_{xx} distributions through the thickness of a plate at the center are depicted in Figs. 3(a) and 3(b) for S=4 and S=10, respectively. The transverse shear stresses obtained by FSDT, EFSDT, and HOZT are plotted and compared in Fig. 4. The legend in Figs. 3-4 is given as follows. The legend 'EFSDT_ansys' indicates an ansys finite element solution based on EFSDT. The legend 'HOZT_FEM' represents a finite element solution based on higher order zig-zag theory (HOZT). The legend 'FSDT' indicates a finite element solution based on a first order shear deformation theory. One can see the discrepancy between an EFSDT and the FSDT, because the shear stiffness of an EFSDT was improved over that of the FSDT via the least-square minimization process. Throughout examples consi-dered for Case I, the results of an EFSDT are well correlated with those of the HOZT.

Case (2): An eight-layer stiffened laminated composite panel [0/90/45/-45/-45/45/90/0] with clamped boundary condition at one side edge under the distributed uniform pressure loading. The dimension of the stiffened composite panel is length a=20 m, width b=14 m, and thickness h=1. Fig. 5 shows the displacement contour of a stiffened composite panel, which is obtained by ANSYS. In Fig. 6, the transverse shear stresses are plotted. It can be seen that the conventional Mindlin-Reissner type shell element denoted by FSDT_anysis in Fig. 6 cannot accurately predict the transverse shear stresses through the thickness of a plate for angle-ply layers. In contrast, an EFSDT and its recovery routine are capable of computing the through-the-thickness distributions of transverse shear stresses accurately.

Case (3): A simply supported $[0^o/\mathrm{Core}/0^o]$ sandwich plate with the thickness of each face sheet equal to h/10 is considered to investigate significant shear deformation effects. The uniform pressure loading is distributed over the whole x-y plane. The in-plane normal and transverse shear stresses are plotted in Figs. 7(a) and 7(b), respectively, for a very thick plate of S=4. The results from an EFSDT are significantly improved over those from the FSDT, as shown in Fig. 7. From this example, one can clearly see that the FSDT is not adequate at all for the analysis of sandwich plates. For more accurate prediction of the transverse shear stresses of a sandwich plate, the ef-

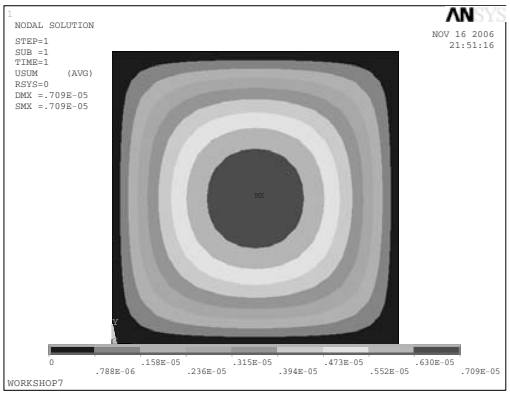

Fig. 2. Displacement contour of rectangular composite plate under uniform loading (S=4).

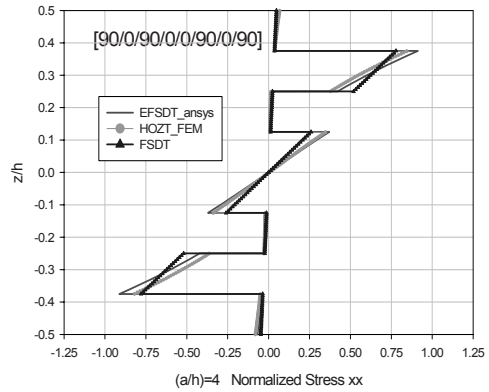

Fig. 3(a). Nondimensional in-plane stress $\sigma_{xx}\left(\overline{\sigma}_x = \sigma_x / q_0 S^2\right)$ under uniform loading.

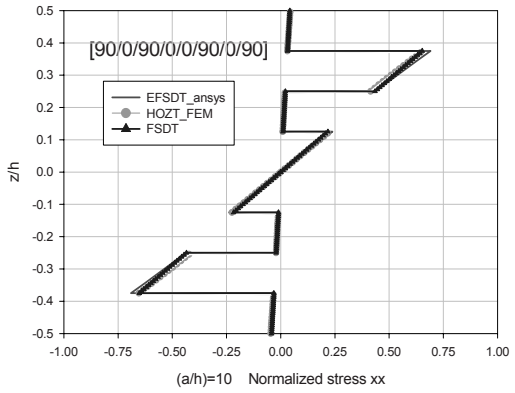

Fig. 3(b). Nondimensional in-plane stress $\sigma_{xx}\left(\overline{\sigma}_x = \sigma_x / q_0 S^2\right)$ under uniform loading.

fect of a transverse normal deformation should be considered. The reason of this is that the core material of a sandwich plate is very flexible as compared to that of the face sheet. Although the proposed approach does not consider the transverse normal effect, it has merit in that it always gives better results than the FSDT while it retains the same computational cost.

Table 1. Center deflection $\overline{u}_3$ under distributed loading.

S=a/h	HOZT_FEM	*EFSDT*	*ANSYS*	*FSDT*
4	2.78	2.77	2.32	2.054
10	1.025	1.025	0.96	0.915

$\overline{u}_3 = u_3 100 E_2 h^3 / (Pa^4)$

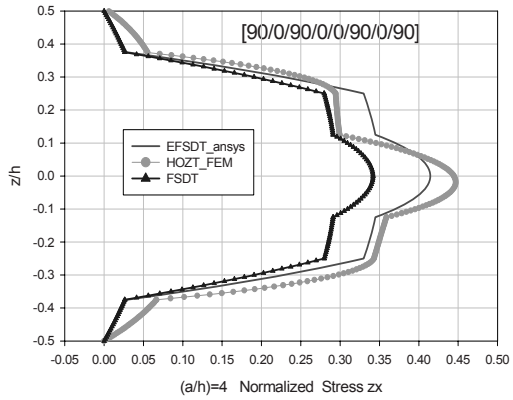

Fig. 4(a). Nondimensional in-plane stress $\sigma_{xx}\left(\overline{\sigma}_x = \sigma_x / q_0 S^2\right)$ under uniform loading.

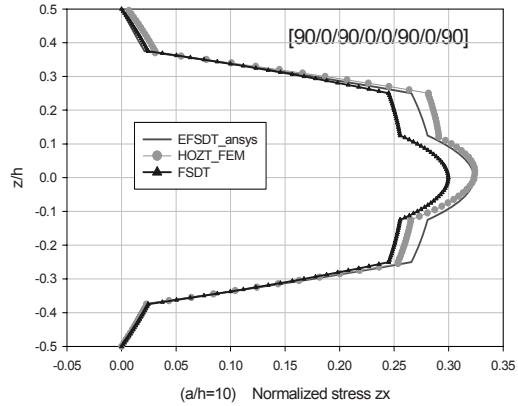

Fig. 4(b). Nondimensional transverse shear stress $\sigma_{zx}\left(\overline{\sigma}_{zx} = \sigma_{zx} / q_0 S\right)$ under uniform loading.

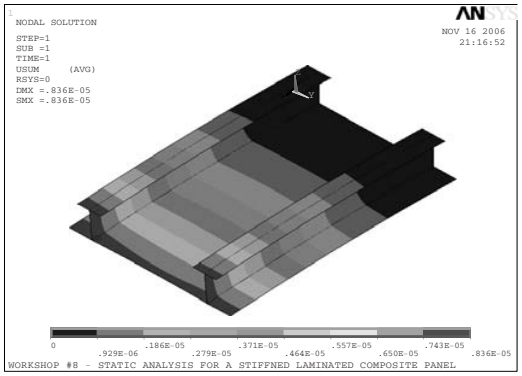

Fig. 5. Displacement contour of stiffened laminated composite panel.

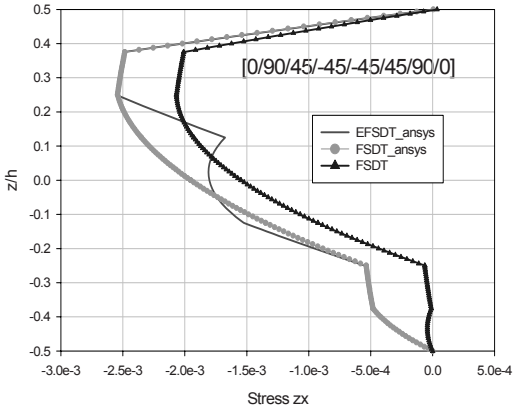

Fig. 6(a). Nondimensional transverse shear stress σ_{zx} under uniform loading.

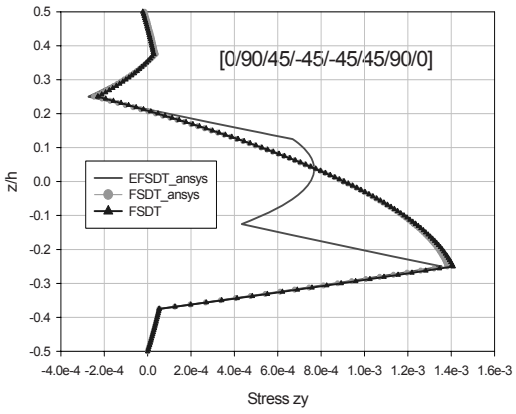

Fig. 6(b). Nondimensional transverse stress σ_{zy} under uniform loading.

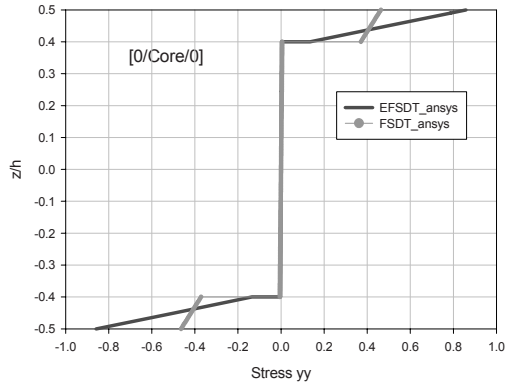

Fig. 7(a). Nondimensional in-plane stress $\sigma_{yy}\left(\overline{\sigma}_y = \sigma_y / q_0 S^2\right)$ of sandwich plate under uniform loading.

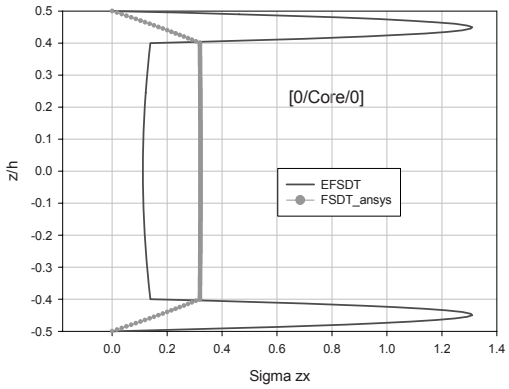

Fig. 7(b). Nondimensional transverse shear stress $\sigma_{zx}\left(\overline{\sigma}_{zx} = \sigma_{zx} / q_0 S\right)$ of sandwich plate under uniform loading.

4. Conclusions

A finite element formulation based on an EFSDT has been developed to predict the behavior of sandwich plates as well as laminated composite plates efficiently and accurately. The displacement fields of the HOZT [1], which is selected for its simplicity and accuracy, are utilized to approximate the through-the-thickness warping functions.

The key feature of the present paper is that the applicability of an EFSDT to the commercial software with virtually no effort is demonstrated. A post-process scheme is developed to calculate the higher order derivatives with respect to in-plane coordinates via the differential quadrature method. This is successfully applied to ANSYS. The accuracy and robustness of the present approach is also demonstrated by analyzing plates with various lay-up configura-

tions including a sandwich plate. The results obtained herein are compared to the FSDT and the HOZT. It is observed that the FSDT severely underestimates the displacements and stresses, whereas the EFSDT shows good agreement with the HOZT. From the numerical examples considered, one can conclude that the proposed finite element formulation provides us with an efficient yet accurate tool for the analysis of laminated composite and sandwich structures without significant modifications to commercial finite element packages.

Acknowledgments

This work was supported by the Korea Foundation for International Cooperation of Science & Technology (KICOS) through a grant provided by the Korean Ministry of Science & Technology (MOST) in No. 2006-00694.

References

[1] M. Cho and R. R. Parmerter, An efficient higher-order plate theory for laminated composites, *Comp. Struc.,* 20 (1985) 113-123.

[2] M. Cho and R. R. Parmerter, Efficient higher order composite plate theory for general lamination configuration, *AIAA Journal,* 31 (7) (1993) 1299-1306.

[3] W. Yu, D. H. Hodges and V. V. Volovoi, Asymptotic construction of Reissner-like composite plate theory with accurate strain recovery, *International Journal of Solids and Structures,* 42 (2002) 6680-6699.

[4] J.-S. Kim and M. Cho, Enhanced modeling of laminated and sandwich plates via strain energy transformation, *Compos. Sci. & Tech.,* 66 (11-12) (2006) 1575-1587.

[5] K. M. Liew, Differential quadrature method for Mindlin plates on Winkler foundations, *Int. J. Mech. Sci.,* 38 (4) (1996) 405-421.

[6] ANSYS, Version 5.6, Canonsburg (PA): SAS IP, USA. (2001).

[7] N. J. Pagano, Exact solutions for rectangular bidirectional composites and sandwich plates, *Journal of Composite Materials,* 3 (1970) 398-441.

[8] K. M. Rao and H. R. Meyer-Piening, Analysis of sandwich plates using a hybrid-stress finite element, *AIAA Journal,* (29) (1991) 1498-1506.